Neuron, Vol. 15, 711–720, September, 1995, Copyright © 1995 by Cell Press

# Glutamate Transporters in Glial Plasma Membranes: Highly Differentiated Localizations Revealed by Quantitative Ultrastructural Immunocytochemistry

**Farrukh A. Chaudhry, Knut P. Lehre, Menno van Lookeren Campagne,* Ole P. Ottersen, Niels C. Danbolt, and Jon Storm-Mathisen**
Anatomical Institute
University of Oslo
N-0317 Oslo
Norway

## Summary

**The glutamate transporters GLT-1 and GLAST were studied by immunogold labeling on ultrathin sections of rat brain tissue embedded in acrylic resins at low temperature after freeze substitution. Both proteins were selective markers of astrocytic plasma membranes. GLT-1 was much higher in hippocampal astrocytes than in cerebellar astrocytes. Astroglial membrane GLAST densities ranked as follows: Bergmann > cerebellar granular layer ≈ hippocampus > cerebellar white matter. No astrocyte appeared unlabeled. Astrocytic membranes facing capillaries, pia, or stem dendrites were lower in glutamate transporters than those facing nerve terminals, axons, and spines. Parallel fiber boutons (glutamatergic) synapsing on interneuron dendritic shafts were surrounded by lower transporter densities than those synapsing on Purkinje cell spines. Our findings suggest the localizations of glutamate transporters are carefully regulated.**

## Introduction

Glutamate uptake is essential for maintaining resting extracellular glutamate concentrations below levels that activate glutamate receptors (Attwell et al., 1993). It is mediated by membrane glycoproteins that also transport other excitatory amino acids (EAAs; Danbolt, 1994). These proteins constitute a gene family (GLAST, Storck et al., 1992; GLT-1, Pines et al., 1992; EAAC1, Kanai and Hediger, 1992), the members of which have distinct distributions in the brain (Danbolt et al., 1992; Levy et al., 1993; Torp et al., 1994; Rothstein et al., 1994; Lehre et al., 1995). When tested under comparable conditions, (the human versions of) three of the proteins have similar affinities for L-glutamate but show differences of more than two orders of magnitude for some other ligands (Arriza et al., 1994), indicating that the different EAA transporters might be accessible to selective pharmacological manipulation.

The occurrence of multiple, differentially distributed EAA uptake carriers, as well as evidence for regulation (Casado et al., 1993; Levy et al., 1995; Trotti et al., 1995), suggests that these proteins have more refined functions than merely clearing the extracellular space of EAAs. They may modify excitation through postsynaptic (Barbour et al., 1994; Mennerick and Zorumski, 1994; Tong and Jahr, 1994) as well as presynaptic (Maki et al., 1994) EAA receptors. Knowledge of the exact location of the different transporters is therefore essential.

We have shown before (Lehre et al., 1995) that GLT-1 and GLAST are localized in astroglial cells and distributed throughout the brain, but at different relative concentrations in different regions. The localization method used then (immunoperoxidase staining of vibratome sections) is not suitable for quantitation or high resolution because of uneven penetration of the immunoreagents and diffusion of the peroxidase reaction product. Here we quantitate, at high resolution, the membrane distributions of GLT-1 and GLAST, avoiding the said problems by using gold particles as label and applying the antibodies directly on ultrathin sections. To preserve both antigenicity and ultrastructure, the tissue was prepared by freeze substitution and low temperature embedding in "antigen friendly" resins (van Lookeren Campagne et al., 1991). The regions highest in GLT and GLAST, hippocampus and cerebellum, were selected for this investigation.

## Results

### Preembedding Immunocytochemistry

A light microscopic survey (Figure 1) revealed that GLT and GLAST were similarly distributed among the different neuropil layers of the hippocampus CA1–CA3, slightly higher in the stratum moleculare of area dentata, and lower in the hilus. The immunoreactivities were somewhat concentrated close to the pyramidal and granular layers, most clearly seen for GLAST, but the pyramidal and granular cells appeared devoid of staining. In the cerebellum, GLT staining intensity was similar in the molecular layer and in the neuropil of the granular layer (i.e., between the granular cell bodies), whereas GLAST was much higher in the molecular layer. Both proteins were found in the special cerebellar astroglial cell type with perikarya (Golgi epithelial cells) located between the (unstained) Purkinje cells and processes (Bergmann fibers) radiating through the molecular layer.

### Postembedding Electron Microscopic Immunocytochemistry

#### *Selective Localization in the Plasma Membranes of Astrocytes*

The maximum particle densities along glial plasma membranes were at least one order of magnitude higher than those along other types of membrane (Table 1). The astroglial membranes recorded in Table 1 were in contact with various other types of membrane, but since none of these showed appreciable labeling in the absence of astrocytic apposition, the labeling could be attributed to the astrocytes. No astrocytic plasma membranes appeared devoid of labeling, indicating that all astrocytes contain GLT and GLAST.

*Present address: F. Hoffmann-La Roche, Pharma Division, Preclinical Research, CH-4002 Basel, Switzerland.

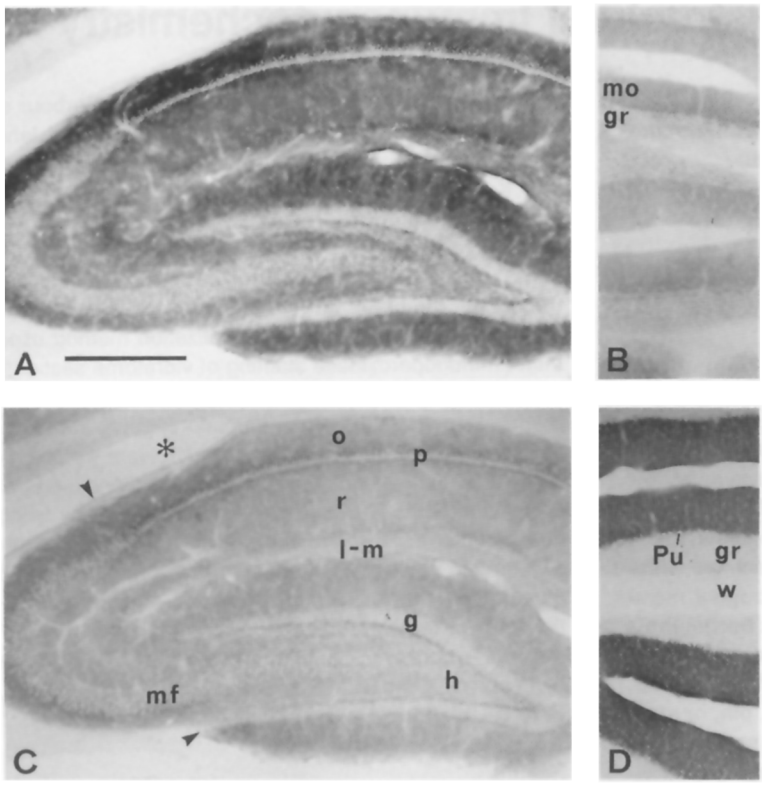


Figure 1. Glutamate Transporters Are Localized in Brain Neuropil and Differently Distributed among Regions

GLT (A and B) is high in hippocampal cortex (A and C), GLAST (C and D) in cerebellar cortex (B and D). Their laminar distributions are similar in hippocampus but different in cerebellum; neuronal perikarya (p, g, and Pu) are unstained (immunoperoxidase with 1 μg/ml αB493 [A and B] or 0.1 μg/ml αA522 [C and D]). Pu, mo, and gr: Purkinje, molecular, and granular layers of cerebellar cortex, respectively; w: white matter; o, p, r, l-m, and mf: stratum oriens, pyramidal cell layer, stratum radiatum, stratum lacunosum-moleculare, and mossy fiber layer of hippocampus, respectively; m, g, and h: molecular, granular, and hilar layers of area dentata, respectively. Arrowheads, borders between CA1 (top right), CA3 (left), and area dentata; asterisk, cerebral ventricle. Bar, 500 μm.

Table 1. Selective Localization of GLT and GLAST in the Plasma Membranes of Astrocytes

| Cell Type | Membrane Type | GLT (α73kDa) | GLAST (αA522) |
|---|---|---|---|
| Astrocytic cell bodies | | | |
| B | Plasmalemmal | | 5.40 ± 0.64 (54) |
| H | | 7.62 ± 0.24 (113) | |
| B | Nuclear | | 0.32 ± 0.07 (10) |
| H | | 0.31 ± 0.06 (17) | |
| B | Mitochondrial | | 0.34 ± 0.22 (6) |
| H | | 0.09 ± 0.05 (30) | |
| B | Endoplasmic | 0.00 (20) | 1.60 ± 0.62 (23) |
| H | Reticulum | 0.40 ± 0.16 (46) | 0.36 ± 0.16 (42) |
| Cerebellar granular cells, apposed | Plasmalemmal | 0.00 (15) | 0.12 ± 0.08 (9) |
| Purkinje cell bodies, apposed to terminals | Plasmalemmal | 0.16 ± 0.11 (19) | 0.09 ± 0.05 (29) |
| Dendrodendritic appositions | | | |
| mo | Plasmalemmal | | 0.19 ± 0.01 (13) |
| l-m | | 0.00 (15) | |
| Axodendritic appositions | | | |
| mo | Plasmalemmal | | 0.17 ± 0.02 (18) |
| l-m | | 0.11 ± 0.08 (42) | |
| Axospinous synapses | | | |
| mo | Synaptic | 0.19 ± 0.13 (34) | 0.40 ± 0.11 (129) |
| l-m | | 0.23 ± 0.14 (89) | 0.24 ± 0.14 (95) |
| r | | 0.53 ± 0.17 (116) | 0.23 ± 0.15 (136) |
| md | | 0.69 ± 0.22 (148) | 0.13 ± 0.13 (121) |

Data are expressed as gold particles per micrometer length of sectioned membrane and given as mean ± SEM (number of profiles in parentheses). For astrocytic profiles, the particle density along the plasma membrane was recorded regardless of the type of neighboring structure. For neuronal profiles, only stretches of plasma membrane apposed to other neuronal membranes, i.e., to nonglial structures, were recorded. For synaptic membranes, 45 nm was excluded at each end to minimize glial contamination. Mitochondrial membranes exclude cristae. In all cases, two membranes were so close together that the particles might belong to anyone of them (see text), but the single length was used throughout to calculate the particle density. B, cell bodies of Bergmann glial fibers in cerebellar cortex; H, hippocampal astrocytes in stratum lacunosum-moleculare; l-m, stratum lacunosum-moleculare of hippocampus CA1; md, stratum moleculare of area dentata; mo, molecular layer of cerebellum; r, stratum radiatum of CA1.

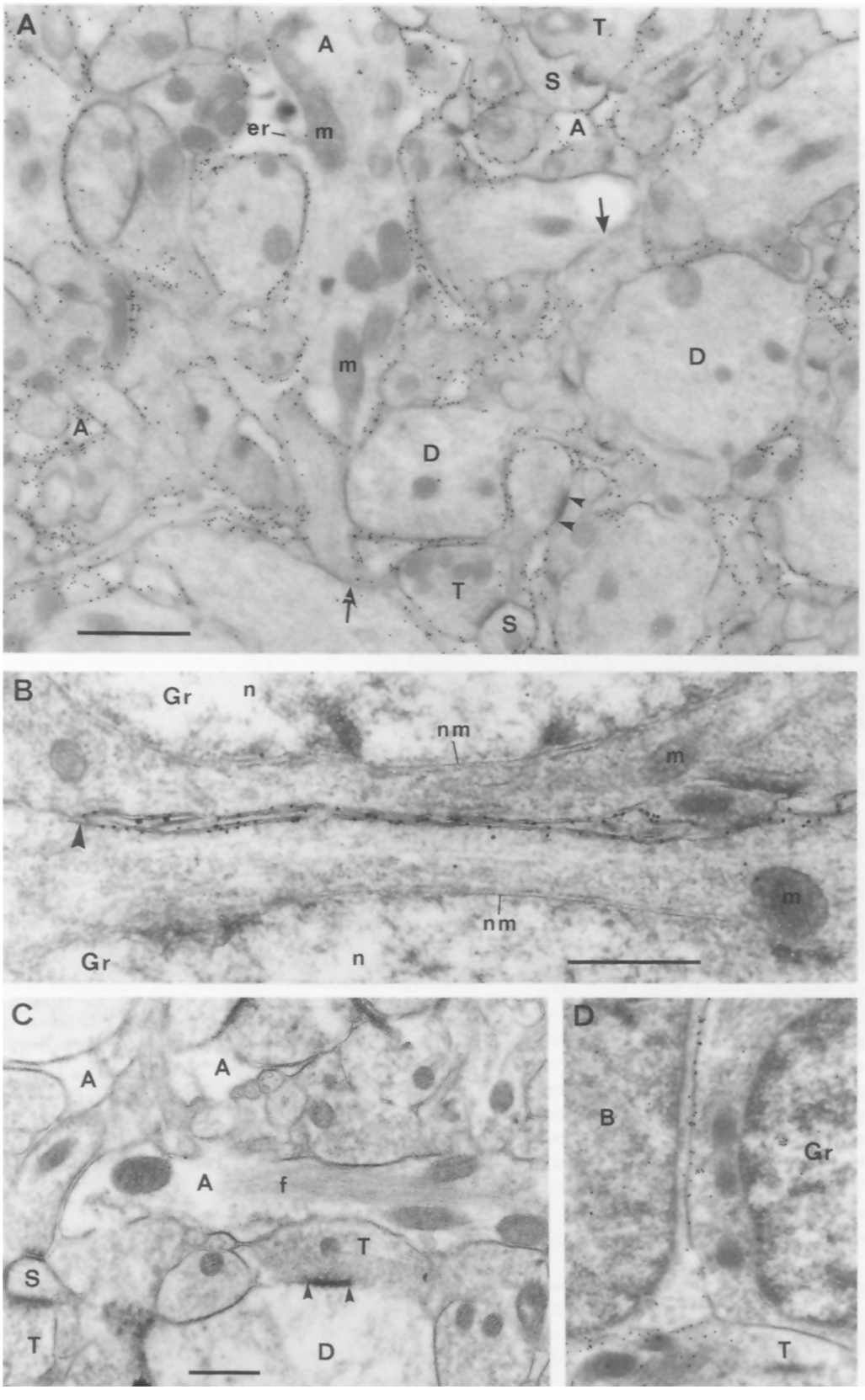


Figure 2. Selective Localization of Glutamate Transporters in Astrocytic Plasma Membranes Revealed by Postembedding Immunocytochemistry

(A) GLT in the neuropil of hippocampus (CA1 stratum lacunosum-moleculare) is associated with astroglial plasmalemmae. Cytoplasmic matrix and membranes of intracellular organelles (er, m, and nm) are almost free of gold particles, as are synaptic membranes (arrowheads) and other neuronal plasma membranes without glial contact (arrows).

(B) GLT-containing glial process penetrating between two granular cell somata (area dentata). The latter lack labeling in the absence of the former (left of arrowhead), suggesting GLT is restricted to the astrocytic plasma membrane (right of arrowhead).

(C) No labeling by control IgG (rest IgG).

(D) GLAST in plasmalemma of an astroglial cell body (B); the membrane of an adjacent cerebellar granular cell (Gr), when not in contact, lacks gold particles.

A, astroglia; B, Golgi epithelial cell (i.e., cell body of Bergmann glial fiber); D, dendrite; er, endoplasmic reticulum; f, glial filaments; Gr, granular cell; m, mitochondria; n, nucleus; nm, nuclear membrane; S, spine; T, nerve terminal. Bars, 1 μm (A and D), 0.5 μm (B and C).

To assess whether the low particle densities along membranes other than astrocytic plasmalemmae are significant, one needs an accurate estimate of background. The outer membrane of astrocytic mitochondria (which presumably are devoid of GLT and GLAST) showed values about 1% (GLT in hippocampus) or 6% (GLAST in cerebellum) of particle densities along astrocytic plasmalemmae (Table 1). Subtracting these values, the astrocytic endoplasmic reticulum (both membranes) had values at 2% (GLT) and 12% (GLAST) of those of astrocytic plasmalemmae. Inspection indicated similarly low levels of the proteins in the Golgi apparatus.

Oligodendrocytic plasma membrane stretches free of astrocytic contact, including the mesaxons and internal surfaces of myelin sheaths, had negligible labeling for both transporters.

Neuronal membranes, when not apposed to astrocytic processes, in most cases showed particle densities at background levels (Table 1; Figure 2; see Figure 4B). Thus, no evidence was obtained for the presence of GLT or GLAST in glutamatergic or nonglutamatergic neurons in general. (The alternative possibility, that neuronal membranes harbor the transporters only where contacting astrocytic membranes, is unlikely since the intracellular antigenic epitopes would then have been revealed by peroxidase immunocytochemistry [see Lehre et al., 1995].)

To investigate whether the transporters could be present in neurons at the synaptic sites, the synaptic membranes of four different types of putative glutamatergic synapse were examined (Table 1). The net GLT particle counts along the synaptic membrane specializations of axospinous synapses in stratum radiatum of hippocampus CA1 and the inner one-third of the stratum moleculare of area dentata approached 10% (averages, 6% and 9%) of the values for astrocytic plasma membranes (subtracting background estimate; see above). Although a large number of synapses was recorded, the total length of membrane and the total number of particles were small; the figures should therefore be interpreted with caution. Nonetheless, selectivity is indicated, since axospinous synapses in stratum lacunosum-moleculare of hippocampus and in the cerebellar molecular layer showed no net particle density for GLT, and none of the synapses examined showed a net labeling for GLAST.

### *Differences between the Distributions of GLT and GLAST*

Different astrocytes showed clear differences in their relative contents of GLT and GLAST (Figure 3). Thus, the GLT and GLAST immunoreactivities in the plasma membranes of Bergmann glia were about 0.25 and 3 times, respectively, that found in the membranes of hippocampal astroglia. Within the cerebellum, GLAST was high in Bergmann glia, low in white matter astrocytes, and intermediate in granular layer astrocytes, the latter showing a GLAST level similar to that of hippocampal astrocytes. On the other hand, GLT showed similar levels in all the observed types of cerebellar astrocyte but was much higher in hippocampal astrocytes.

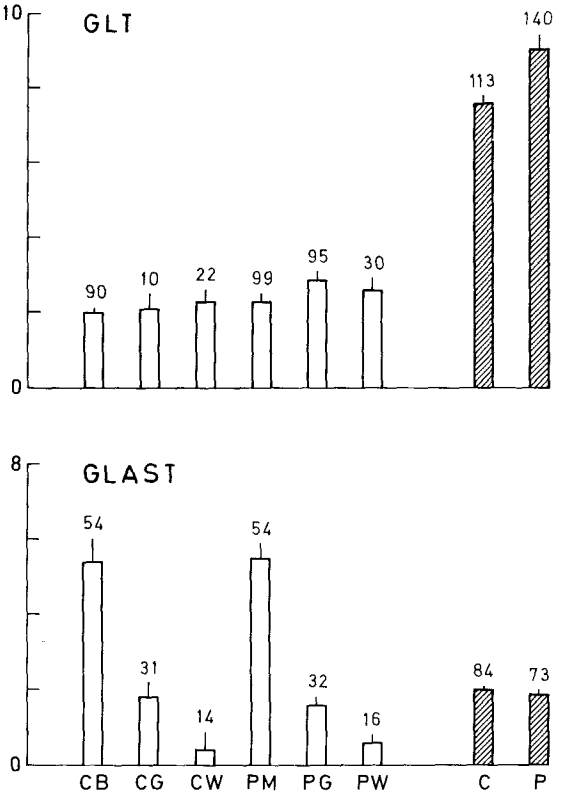


Figure 3. Quantitation of Glutamate Transporters in the Plasma Membranes of Different Categories of Astrocyte

Gold particles per micrometer of membrane length (mean + SEM; number of profiles over columns) were measured along transected plasma membrane profiles. Histograms show a highly differentiated distribution of GLAST but not GLT in the cerebellum and show the reverse distributions of the two proteins between cerebellum (open columns) and hippocampus (hatched columns). CB, cell bodies of Bergmann glial fibers; CG, cell bodies of astrocytes in the cerebellar granular layer; CW, cell bodies of astrocytes in the white matter of cerebellar folia; PM, PG, and PW, astrocytic processes in the cerebellar molecular layer, granular layer, and white matter, respectively; C and P, astrocytic cell bodies and processes in the hippocampus CA1 stratum lacunosum-moleculare. Statistics: for GLT, C ≠ P ≠ all other sites; for GLAST, CB and PM ≠ all other sites ($p < .0001$, ANOVA/Student–Newman–Keul); for GLAST, CG and PG ≠ CW and PW ($p = .02$ and $p = .003$, Wilcoxon rank-sum).

### *Differences between Regions of the Astrocytic Plasma Membranes*

The general labeling densities of the membranes of filament-containing glial processes differed only slightly from those of astrocytic perikarya (Figure 3) or the finest astroglial processes (apposed to axon terminals and dendritic spines; see Figure 5). There were, however, differences related to the type of adjacent structure. Most conspicuously, the region of astrocytic membrane adjoining the basal lamina surrounding capillary endothelium was less immunoreactive than that facing the neuropil (Figure 4A; Figure 5). Similar differences were observed between the neuropil-facing and the opposite surfaces of glial processes contacting the pia, or large dendrites of Purkinje

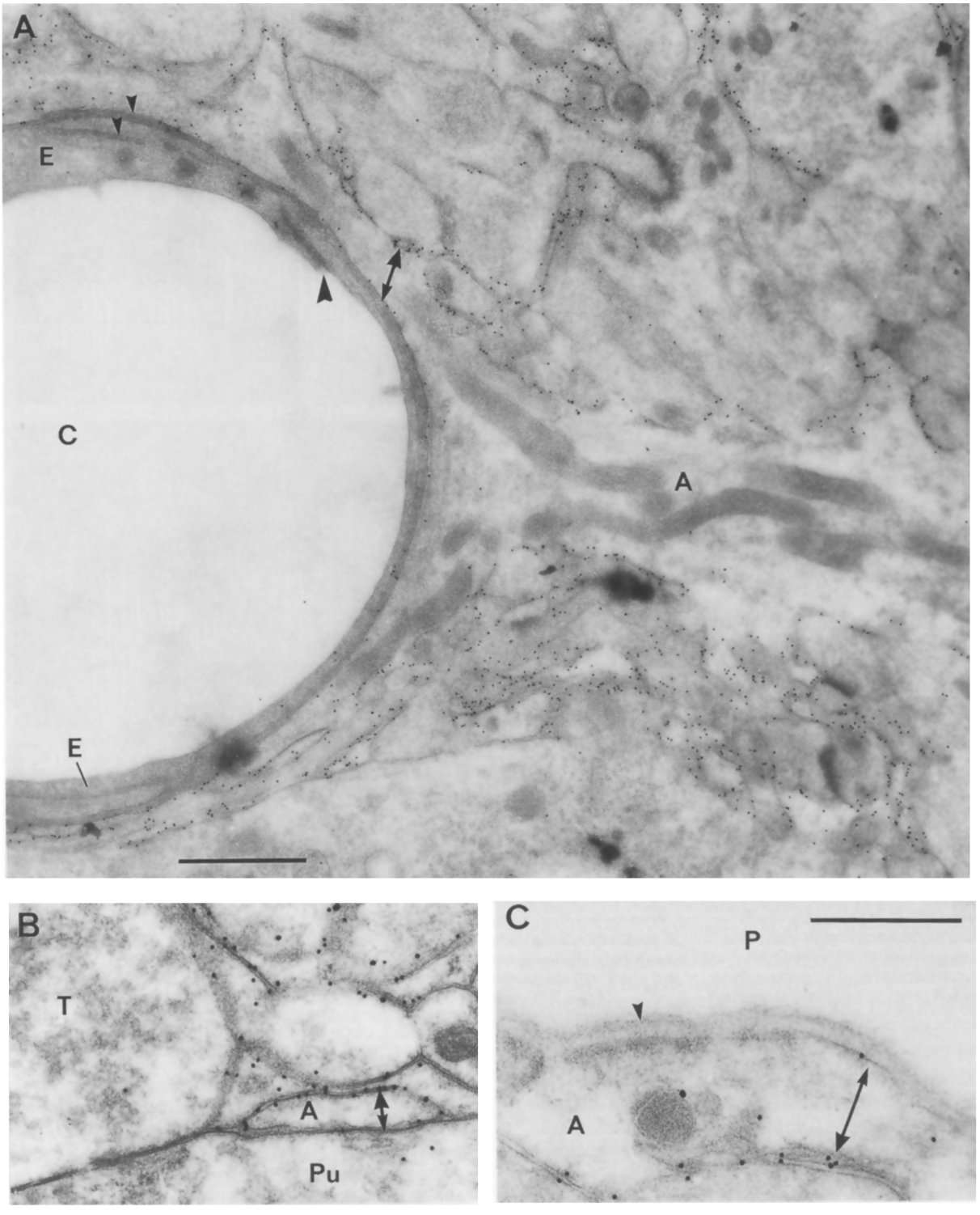


Figure 4. Glutamate Transporters Show Differential Localization among Different Regions of the Same Astrocytic Plasma Membrane

(A) GLT-immunoreactive astroglial process surrounding blood vessel (area dentata). The abluminal membrane facing the neuropil is more intensely labeled (double arrow) than the luminal membrane of the same glial process.

(B) The membrane regions of glial processes contacting Purkinje cells have reduced GLAST compared (double arrow) with those facing neuropil. The apposed plasma membranes of the Purkinje cell and a somatic (likely inhibitory, GABAergic) terminal are free of particles.

(C) The pia-facing membrane of an astrocytic process has less GLAST (double arrow) than the neuropil-facing membrane (cerebellar cortex). A, astroglial process; C, capillary lumen; E, endothelial cell; P, pia mater; Pu, Purkinje cell; T, nerve terminal. Small arrowheads, basal lamina; large arrowhead, junction between endothelial cells. Bars, 1 μm (A), 0.5 μm (B and C).

cells (Figure 4C; Figure 5). Inspection also indicated similar differences for the opposite surfaces of astrocytic processes contacting GABAergic perikarya (Figure 4B), pyramidal cells, or oligodendrocytes. These differences were observed for GLT as well as for GLAST in both cerebellum and hippocampus, but varied in magnitude.

On the other hand, there was no clear difference in GLT or GLAST between astrocytic membranes contacting the presynaptic versus the postsynaptic elements of putative glutamatergic synapses (Figure 5). These membranes had about the same particle densities as astrocytic membranes contacting neuropil elements in general. Astroglial processes apposed to the putative GABAergic synapses contacting Purkinje cell bodies also showed particle densities similar to those on astrocytic membranes in the surrounding neuropil (1.8 ± 0.3 GLT particles per micrometer and 5.8 ± 1.3 GLAST particles per micrometer [mean ± SEM]; n = 33 and 12 profiles, respectively; see Figure 5).

Interestingly, these particle densities were about the same as those observed along the two apposed membranes of astrocytic processes lying in direct contact with each other (Figure 5). Since the resolution of the present method does not allow individual gold particles to be assigned to one of the two membranes, it follows that the GLT and GLAST immunoreactivities at astrocytic membranes contacting other astrocytic membranes are about 50% of those at astrocytic membranes contacting neuronal elements.

### *Localization in the Vicinity of Identified Glutamatergic Synapses with Different Functional Properties*

The distributions of GLAST and GLT differed dramatically at two functionally different (Barbour et al., 1994) categories of glutamatergic synapse (Figure 6; Figure 7), made by parallel fiber boutons in the cerebellar molecular layer. To estimate the availability of EAA uptake sites for removal of glutamate immediately after synaptic release, the distance was measured along the cut intercellular cleft from the midpoint of the synaptic specialization to individual immunogold particles. Both the histogram distribution and the cumulated particle number within 1 μm showed far more particles for the spine than for the shaft synapses. This is partly an effect of the steric arrangement of astrocytic profiles, as the mean distance to the nearest astrocytic membrane was much shorter for the spine than for the shaft synapses. However, the immunogold particle density recorded along the 1 μm stretch of astrocytic membrane nearest the synapse in the plane of sectioning was higher for the spine than for the shaft synapse (2 specimens analyzed for GLAST, 1 for GLT; $p < .002$ in each case, Wilcoxon rank-sum test). The spine value was close to that along glial processes facing neuropil in general (see Figure 5).

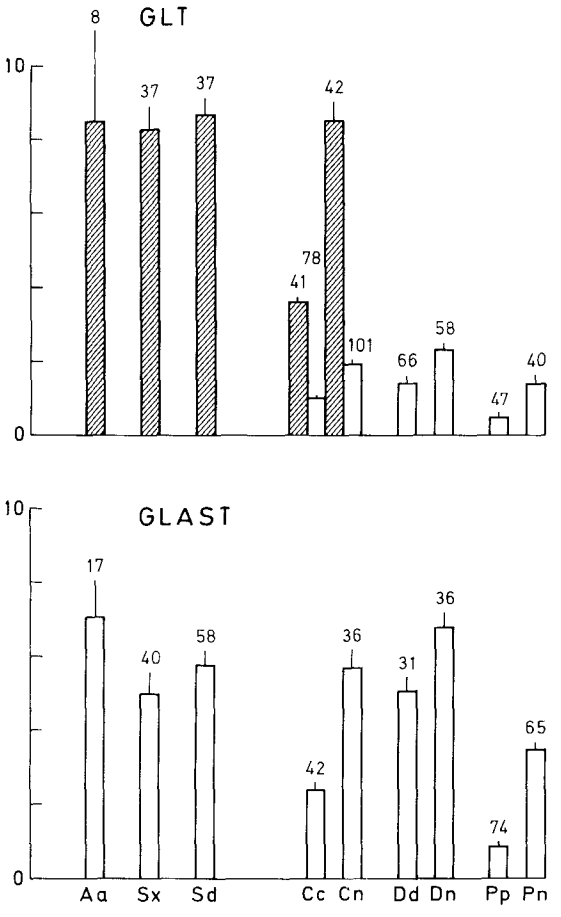


Figure 5. Quantitation of Glutamate Transporters in Different Regions of Astrocytic Membranes

Data (gold particles per micrometer of membrane length) were obtained and presented as in Figure 3 (hatched bars, hippocampus; open bars, cerebellum). The apposed membranes of two astrocytic processes (at least one of which contained filaments; Aa) together have less than twice the particle density of single astrocytic membranes apposed to other neuropil elements in the vicinity (Sx and Sd). Astrocytic plasma membranes apposed to the presynaptic (Sx) and postsynaptic (Sd) element of axospinous synapses do not differ in GLT or GLAST. Astrocytic membranes facing the basement laminae of capillaries (Cc) or pia (Pp) or Purkinje cell dendritic shafts (Dd) are all lower in GLT and GLAST than are the membranes of the same glial processes facing adjacent neuropil elements (Cn, Dn, and Pn). Statistics: for GLT, Cc/Cn hippocampus ($p < .0001$), cerebellum ($p = .04$); for GLAST, Cc/Cn and Pp/Pn ($p < .0001$), Dd/Dn ($p = .01$; ANOVA/Student–Newman–Keul).

## Discussion

### Cellular Localization

Here we show by quantitative postembedding immunocytochemistry that the EAA transporters GLT-1 and GLAST are localized in the plasma membranes of astrocytes. This extends previous findings based on preembedding immunocytochemistry (Danbolt et al., 1992; Levy et al., 1993; Rothstein et al., 1994; Lehre et al., 1995) and on in situ hybridization (Storck et al., 1992; Torp et al., 1994). At the regional level, our data are in excellent agreement with quantitative Western blotting (Lehre et al., 1995). Although no calibration was made, this indicates that the immunogold particle density faithfully reflects the protein concentration in the membranes.

Our immunogold quantitation suggested that the transporters may not be expressed at all, or at very low levels, in most neuronal membranes. However, the synaptic membranes of some excitatory, putative glutamatergic

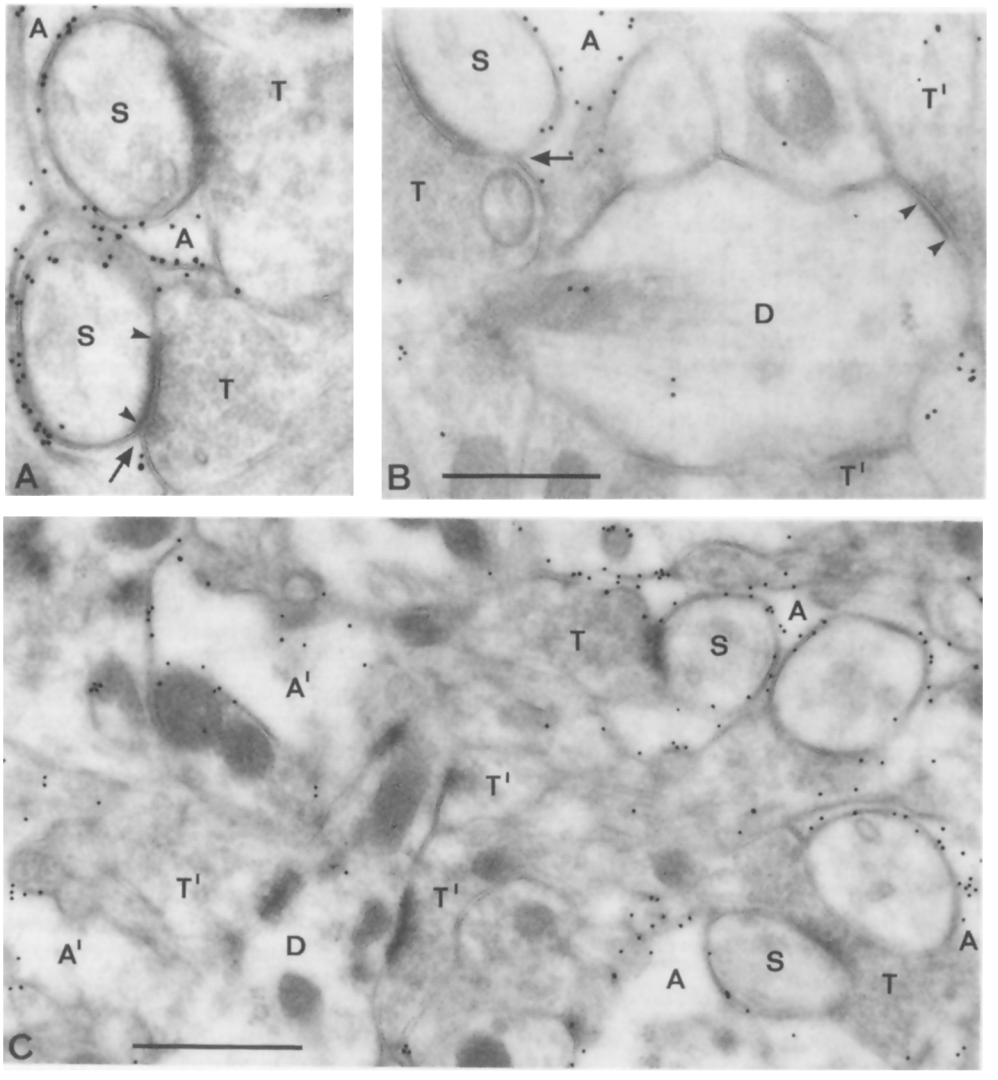


Figure 6. Differential Glutamate Transporter Localization at Two Types of Glutamatergic Synapse with Different Functional Properties

In the cerebellar molecular layer, parallel fiber boutons synapsing on spines, i.e., on Purkinje cells (A), are more closely surrounded by GLAST-labeled glial processes than are parallel fiber boutons synapsing on dendritic shafts, i.e., on interneurons (B). The difference is evident at low magnification (C). The distance between the synaptic site and the closest glial process (arrows) is shorter at the spine synapses than at the shaft synapses. The particle density also appears lower in parts of glial processes (A′) close to shaft synapses than in ones close to spine synapses. A, astroglial process; A′, astroglial process in proximity to shaft synapses; D, dendritic shaft; S, dendritic spine; T, nerve terminal synapsing on spine; T′, nerve terminal synapsing on dendritic shaft. Arrowheads, extents of synaptic membrane specializations. Bars, 0.5 μm (A and B), 1 μm (C).

synapses in the hippocampus showed net particle densities indicating GLT contents on the order of 5%–10% of the astrocytic values. This was not detected by preembedding electron microscopic immunocytochemistry (Danbolt et al., 1992; Lehre et al., 1995). Although the signals are too low to draw firm conclusions, they indicate the possible presence of some GLT at the synapses formed by the terminals of Schaffer collaterals (from CA3 pyramidal cells) and axons from hilar (CA4) mossy cells. This would be consistent with the observation of GLT-1 mRNA in the parent neuronal perikarya (Torp et al., 1994; our unpublished data). The fact that hippocampal levels of GLT protein are much lower in neurons than in astrocytes may be due to posttranscriptional block of protein synthesis in the neurons (or perhaps posttranslational modification precluding recognition by the antibodies). Since neither GLT nor GLAST, nor EAAC1 (Rothstein et al., 1994), seem to be expressed at appreciable levels in hippocampal excitatory terminals, which have high EAA uptake activities (Gundersen et al., 1993), the terminals may contain a different EAA transporter yet to be identified.

Using an antibody directed against GLAST amino acid residues 504–518, Rothstein et al. (1994) reported staining of glutamatergic (e.g., hippocampal pyramidal and granular) as well as nonglutamatergic (e.g., Purkinje) neurons in addition to astrocytic processes. Since the neuronal staining appeared localized to the Golgi apparatus rather than the plasmalemma, the authors suggested that GLAST protein might be incorporated into the plasma membranes of neurons after cleaving off of a C-terminal

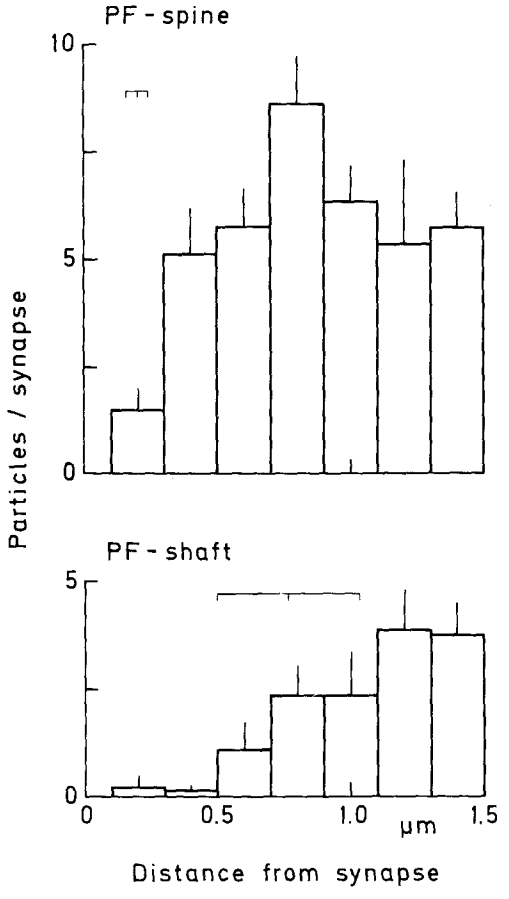


Figure 7. Quantitation of Glutamate Transporter Distribution Relative to Parallel Fiber–Dendritic Spine and Parallel Fiber–Dendritic Shaft Synapses

Columns represent mean numbers of particles signaling GLAST (bars indicate SEM; 8 parallel fiber–spine synapses and 8 parallel fiber–shaft synapses). Positions along the horizontal axis represent the distances to the particles (i.e., the points of projection onto the intercellular cleft) from the midpoint of the synaptic complex, measured along the intercellular clefts. All of the shaft synapses had fewer particles within 1.0 μm than any of the spine synapses (5.1 ± 1.1 and 24.5 ± 2.1, mean ± SEM; $p < .001$, Wilcoxon rank-sum). Horizontal brackets indicate the distance (mean ± SEM) from the midpoint of the synapse to the nearest astrocytic membrane, in all cases longer for the shaft than for the spine synapses ($p < .001$). The particle density at this astrocytic membrane (recorded along a 0.5 μm stretch in each direction from the closest point) was lower for the shaft than for the spine synapses (3.1 ± 0.6 and 6.5 ± 0.6 particles/μm; $p = .001$). The former was also lower than the particle density along astrocytic membranes apposed to nonsynaptic regions of parallel fibers (16) in the same fields (5.5 ± 0.6 particles/μm; $p = .01$). Background (not subtracted) was 0.27 ± 0.04 particles/μm, as estimated along apposed parallel fiber membranes in each of the observed fields (7).

fragment including amino acid residues 504–518. This, however, seems unlikely, as a GLAST antibody specific to residues 3–14, as well as one specific to residues 522–541 (αA522), failed to label neurons but produced strong labeling of astrocytes (Lehre et al., 1995). Furthermore, GLAST mRNA has not been detected in neurons (Storck et al., 1992; Torp et al., 1994). Therefore, a different explanation should be sought for the staining of neuronal perikarya reported by Rothstein et al. (1994).

### Differential Localization in the Plasma Membranes of the Same Astrocytes

An important finding of the present investigation is the differential distribution of GLT and GLAST along the plasma membranes of the same glial cells. Such a differential localization of solute transporters has to our knowledge not previously been reported in cells lacking zonulae occludentes. The results suggest that the density of transporter molecules is highest in synaptic regions as opposed to regions of presumably lower demand, i.e., dendritic stems, vascular endothelium, pial surface, and apposed astrocytic membranes. The most peculiar is the differentiation in transporter density between Bergmann glial processes neighboring on synapses by cerebellar parallel fibers onto two different postsynaptic sites (see below). Relative to these two targets, the glial processes thus show differences in chemistry as well as in architecture.

### Localization Relative to Synapses of Different Properties: Functional Roles

Our findings provide an explanation for the recent observations that different glutamatergic synapses show different sensitivities to EAA transport inhibitors. Several such inhibitors prolong the synaptic current at parallel fiber synapses onto Purkinje cell spines, but not at those onto interneuron dendritic shafts (Barbour et al., 1994). We have shown that EAA transporter–containing astrocytic membranes surround the former type of synapse much more closely than the latter. The relation between receptor activation and desensitization depends on the time course and amplitude of the extracellular glutamate concentration (Barbour et al., 1994). In addition, there is evidence for regulation of synaptic glutamate release (by presynaptic receptors; Maki et al., 1994) and of glial glutamate release (Attwell, 1994). These mechanisms form a rationale for maintaining a differential distribution of EAA transporters, as observed here. The findings go together with evidence of regulation of EAA transporter activity (Casado et al., 1993; Levy et al., 1995; Trotti et al., 1995), and with the very existence of different transporter protein species, to suggest that these proteins may carefully tune the extracellular glutamate concentration to achieve appropriate functional activation of EAA receptors.

## Experimental Procedures

### Tissue Preparation

Rats were perfusion fixed (Lehre et al., 1995) with a solution of 2.5% glutaraldehyde, 1% (para)formaldehyde in 0.1 M phosphate buffer (pH 7.4), except for the experiment in Figure 1 (4% formaldehyde, 0.2% picric acid, 0.05% glutaraldehyde). For freeze substitution <0.3 $mm^3$ blocks were processed by procedure A or B, with similar results. Gold-colored ultrathin sections were cut and mounted on nickel mesh grids.

For procedure A, samples from 6 rats were cryoprotected (30% glycerol in phosphate buffer) and frozen in liquid propane at −190°C in a cryofixation unit (KF80, Reichert-Jung, Austria). The tissue was freeze substituted with 0.5% uranyl acetate in 100% methanol in a cryosubstitution unit (CS Auto or AFS, Reichert) and embedded in Lowicryl HM20 (Lowi, Switzerland) (Müller et al., 1980; van Lookeren Campagne et al., 1991).

For procedures B, tissue from 2 rats (in 1-hexadecene) was frozen by a high pressure freezer (HPM 010, Balzers, Lichtenstein) without

cryoprotection (Studer et al., 1989), freeze substituted with 0.5% uranyl acetate in 100% ethanol in a FSU 010 unit (Balzers), and embedded in Lowicryl HM23 (Lowi).

### Antibodies

The antibody preparation α73kDa was raised and affinity isolated as described (Danbolt et al., 1992) against EAA transporter protein purified from rat brain (Danbolt et al., 1990), then used to clone GLT-1 (Pines et al., 1992; corrected sequence from Kanner, 1993). It reacts strongly with GLT-1 amino acid residues 493–508 (Levy et al., 1993). The antibodies αB12, αB493, and αA522 were raised, purified, and characterized as described (Lehre et al., 1995). Control IgG was isolated from the α73kDa serum after extensive absorption on the affinity column to extract all α73kDa antibody (Danbolt et al., 1992).

### Immunocytochemistry

Preembedding immunocytochemistry was performed as described (Lehre et al., 1995) with detergent Triton X-100 to minimize staining differences due to different penetration of immunoreagents. For postembedding immunocytochemistry, the ultrathin sections were processed (based mainly on van Lookeren Campagne et al., 1991; Phend et al., 1992) at room temperature in solutions containing 50 mM Tris–HCl (pH 7.4), 0.9% NaCl, and 0.1% Triton X-100 (TBST), with additions as stated. The sections were washed in TBST containing 0.1% $NaBH_4$ and 50 mM glycine (10 min) and then in TBST containing 3% human serum albumin. They were incubated overnight with primary antibody (4.7 μg/ml αA522, 5.0 μg/ml α73kDa, 5.5 μg/ml αB493, and 40 μg/ml αB12 [final concentrations]; no net gain in signal at higher concentrations) in TBST/HSA. The localization of GLT appeared the same with all three antibodies; since αB12 and αB493 gave weaker signals, α73kDa was used for the detailed analysis. Control IgG at the same concentrations gave no labeling. Bound antibodies were visualized by 15 nm gold-labeled goat anti-rabbit Ig (GAR15, Amersham, England). The sections were contrasted by uranyl acetate and lead citrate and observed in a Phillips CM10 electron microscope.

### Analysis

The qualitative observations described were made consistently in all specimens examined (up to 6 each from hippocampus and cerebellum). For quantitation, pictures were printed at 48,500×. The lengths of stretches of transected membrane were measured by means of a digitizing tablet, and the densities of the associated gold particles were computed.

The distribution of particles with distance from the labeled membranes was tested in astrocytic processes since astrocytes, according to the peroxidase immunocytochemistry, appeared to be the only immunoreactive structures. The cerebellar molecular layer was examined after labeling for GLAST. Out of 692 particles located within ± 60 nm of the midline of an astrocytic plasma membrane apposed to a neuronal one, 63% had their centers within ± 20 nm and 89% within ± 40 nm. Less than 5% of the additional particles were found between ± 60 and ± 80 nm. The distribution was rather symmetrical around the midline of the glial plasma membrane; i.e., it did not show which side of the membrane the antigenic epitopes were on, but suggested that the epitopes were scarce in the adjacent neuronal membrane. Hence, particles within 45 nm were recorded.

For the data presented in Figure 7, the distances and the lengths of membrane profiles were measured by a cartographic hodometer (reproducible within 10 nm in the range of 100–300 nm). Asymmetric synapses on dendritic shafts (i.e., on interneurons) were identified in the cerebellar molecular layer (Palay and Chan-Palay, 1974). All those encountered were analyzed together with a nearby asymmetric synapse on a dendiritic spine (i.e., on a Purkinje cell). Both types are almost exclusively formed by parallel fibers.

### Acknowledgments

We are indebted to A. Verkleij, J. Boonstra, and B. Humbel, University of Utrecht, and to M. Müller and P. Walter, Federal Institute of Zürich, for advice and for the permission to use laboratory facilities. Thanks are also due to K. M. Gujord, C. Knudsen, G. F. Lothe, T. Nordby, B. Riber, and K. Ruud for assistance, and to T. Eid and N. Roos for discussion. This work was supported by the Norwegian Research Council, an EU Concerted Action (BMH1-CT94–1248), the Jahre Fund, and a private donation. Correspondence should be addressed to J. S.-M.

The costs of publication of this article were defrayed in part by the payment of page charges. This article must therefore be hereby marked *"advertisement"* in accordance with 18 USC Section 1734 solely to indicate this fact.

Received March 13, 1995; revised May 30, 1995.

### References

Arriza, J. L., Fairman, W. A., Wadiche, J. I., Murdoch, G. H., Kavanaugh, M. P., and Amara, S. G. (1994). Functional comparisons of three glutamate transporter subtypes cloned from human motor cortex. J. Neurosci. *14*, 5559–5569.

Attwell, D. (1994). Glia and neurons in dialogue. Nature *369*, 707–708.

Attwell, D., Barbour, B., and Szatkowski, M. (1993). Nonvesicular release of neurotransmitter. Neuron *11*, 401–407.

Barbour, B., Keller, B. U., Llano, I., and Marty, A. (1994). Prolonged presence of glutamate during excitatory synaptic transmission to cerebellar Purkinje cells. Neuron *12*, 1331–1343.

Casado, M., Bendahan, A., Zafra, F., Danbolt, N. C., Aragón, C., Giménez, C., and Kanner, B. I. (1993). Phosphorylation and modulation of brain glutamate transporters by protein kinase C. J. Biol. Chem. *268*, 27313–27317.

Danbolt, N. C. (1994). The high affinity uptake system for excitatory amino acids in the brain. Prog. Neurobiol. *44*, 377–396.

Danbolt, N. C., Pines, G., and Kanner, B. I. (1990). Purification and reconstitution of the sodium- and potassium-coupled glutamate transport glycoprotein from rat brain. Biochemistry *29*, 6734–6740.

Danbolt, N. C., Storm-Mathisen, J., and Kanner, B. I. (1992). A [$Na^+$ + $K^+$]coupled -glutamate transporter purified from rat brain is located in glial cell processes. Neuroscience *51*, 295–310.

Gundersen, V., Danbolt, N. C., Ottersen, O. P., and Storm-Mathisen, J. (1993). Demonstration of glutamate/aspartate uptake activity in nerve endings by use of antibodies recognizing exogenous D-aspartate. Neuroscience *57*, 97–111.

Kanai, Y., and Hediger, M. A. (1992). Primary structure and functional characterization of a high-affinity glutamate transporter. Nature *360*, 467–471.

Kanner, B. I. (1993). Glutamate transporters from brain—a novel neurotransmitter transporter family. FEBS Lett. *325*, 95–99.

Lehre, K. P., Levy, L. M., Ottersen, O. P., Storm-Mathisen, J., and Danbolt, N. C. (1995). Differential expression of two glial glutamate transporters in the rat brain: quantitative and immunocytochemical observations. J. Neurosci. *15*, 1835–1853.

Levy, L. M., Lehre, K. P., Roístad, B., and Danbolt, N. C. (1993). A monoclonal antibody raised against an [$Na^+$ + $K^+$]coupled -glutamate transporter purified from rat brain confirms glial cell localization. FEBS Lett. *317*, 79–84.

Levy, L. M., Lehre, K. P., Walaas, S. I., Storm-Mathisen, J., and Danbolt, N. C. (1995). Down-regulation of glial glutamate transporters after glutamatergic denervation in the rat brain. Eur. J. Neurosci., in press.

Maki, R., Robinson, M. B., and Dichter, M. A. (1994). The glutamate uptake inhibitor L-trans-pyrrolidine-2,4-dicarboxylate depresses excitatory synaptic transmission via a presynaptic mechanism in cultured hippocampal neurons. J. Neurosci. *14*, 6754–6762.

Mennerick, S., and Zorumski, C. F. (1994). Glial contributions to excitatory neurotransmission in cultured hippocampal cells. Nature *368*, 59–62.

Müller, M., Marti, T., and Kriz, S. (1980). Improved structural preservation by freeze-substitution. Proc. 7th Eur. Congr. Electron Microsc. *2*, 720–721.

Palay, S. L., and Chan-Palay, V. (1974). Cerebellar Cortex: Cytology and Organization (Berlin: Springer-Verlag).

Phend, K. D., Weinberg, R. J., and Rustioni, A. (1992). Techniques to optimize post-embedding single and double staining for amino acid neurotransmitters. J. Histochem. Cytochem. *40*, 1011–1020.

Pines, G., Danbolt, N. C., Bjørås, M., Zhang, Y., Bendahan, A., Eide, L., Koepsell, H., Storm-Mathisen, J., Seeberg, E., and Kanner, B. I. (1992). Cloning and expression of a rat brain L-glutamate transporter. Nature *360*, 464–467. Comments: 420–421.

Rothstein, J. D., Martin, L., Levey, A. I., Dykes-Hoberg, M., Jin, L., Wu, D., Nash, N., and Kuncl, R. W. (1994). Localization of neuronal and glial glutamate transporters. Neuron *13*, 713–725.

Storck, T., Schulte, S., Hofmann, K., and Stoffel, W. (1992). Structure, expression, and functional analysis of a $Na^+$-dependent glutamate/aspartate transporter from rat brain. Proc. Natl. Acad. Sci. USA *89*, 10955–10959.

Studer, D., Michel, M., and Müller, M. (1989). High pressure freezing comes of age. Scanning Micr. Suppl. *3*, 253–269.

Tong, G., and Jahr, C. E. (1994). Block of glutamate transporters potentiates postsynaptic excitation. Neuron *13*, 1195–1203.

Torp, R., Danbolt, N. C., Babaie, E., Bjørås, M., Seeberg, E., Storm-Mathisen, J., and Ottersen, O. P. (1994). Differential expression of two glial glutamate transporters in the rat brain: an *in situ* hybridization study. Eur. J. Neurosci. *6*, 936–942.

Trotti, D., Volterra, A., Lehre, K. P., Rossi, D., Gjesdal, O., Racagni, G., and Danbolt, N. C. (1995). Arachidonic acid inhibits a purified and reconstituted glutamate transporter directly from the water phase and not via the phospholipid membrane. J. Biol. Chem. *270*, 9890–9895.

van Lookeren Campagne, M., Oestreicher, A. B., van der Krift, T. P., Gispen, W. H., and Verkleij, A. J. (1991). Freeze-substitution and Lowicryl HM20 embedding of fixed rat brain: suitability for immunogold ultrastructural localization of neural antigens. J. Histochem. Cytochem. *39*, 1267–1279.